MultiScience - XXXI. microCAD International Multidisciplinary Scientific Conference
University of Miskolc, Hungary, 20-21 April 2017
ISBN 978-963-358-132-2

NUMERICAL SIMULATION OF FLOW AND HEAT TRANSFER FOR A CYLINDER IN FREE VIBRATION

Dániel Dorogi [1]**,** ***László Baranyi*** [2]
[1] PhD student, [2] Professor
[1,2] *Department of Fluid and Heat Engineering, Institute of Energy Engineering and Chemical Machinery, University of Miskolc, Hungary*

ABSTRACT

This study deals with the numerical investigation of two-dimensional, Newtonian fluid flow around and heat transfer from a circular cylinder undergoing one-degree-of-freedom free vibration. The governing equations with the boundary and initial conditions are solved using the finite difference method. During the computations mass ratio, structural damping and Reynolds number are kept at constant values of m^*=10, ζ=0.01 and Re=200, respectively, and the reduced velocity is varied in the range of U^*=4–7. Since a newly extended in-house code is applied, validation is required; computational results compare well with those available in the literature. Besides force coefficients, the mechanical energy and heat transfer between the cylinder and the fluid are also investigated. Large heat transfer and mechanical energy values are obtained near the maximum amplitude of cylinder oscillation.

INTRODUCTION

Fluid flow around an oscillating circular cylinder is frequently investigated using both experimental and numerical approaches. When a structure is exposed to wind or wave, vortices shedding from the body periodically can induce high amplitude vibrations. The motion can be one-degree-of-freedom (1DoF), where the cylinder is restricted to move only in one direction (streamwise or transverse), or two-degree-of-freedom (2DoF), where the body is allowed to move in both directions.

In this study free vibration of an elastically supported cylinder is investigated. Non-dimensional parameters are introduced, namely mass ratio m^*, structural damping ζ and reduced velocity U^*. Their definitions can be found in e.g. [1]. Mass ratio and structural damping are often combined, resulting in the mass-damping parameter $m^*\zeta$. Several studies [1–3] investigated 1DoF motion at medium Reynolds numbers (Re=$U_\infty d/\nu$, where U_∞ is the freestream velocity, d is the cylinder diameter and ν is the kinematic viscosity) using experimental approaches. It was shown that $m^*\zeta$ highly influences the cylinder response: with high $m^*\zeta$ only two branches exist (initial and lower), in contrast with low $m^*\zeta$, where three branches (initial, upper and lower) are observed. Low Reynolds numbers are rarely investigated using experimental approaches. Anagnostopulos and Bearman [4] investigated the $90 < \mathrm{Re} < 150$ regime and found that the highest amplitudes are near the lower limit of lock-in (where the cylinder oscillation synchronizes with the vortex shedding). Their results are compared with numerical studies, e.g., with [5], and good agreement was observed. The branching behavior of VIV (vortex-induced vibration) was investigated numerically at Re=200 with $m^*\zeta$=0.01 and a critical U^*

value was found at which the vibration amplitude is high and afterwards slightly decreases [6]. A study of mass and damping effects found that with increasing $m^*\zeta$ the locked-in regime decreases [7].

Heat transfer also plays an important role in many engineering applications (e.g. chimneys, transmission lines, and heat exchangers). Heat transfer from a stationary cylinder has been extensively studied (e.g [8] and [9]), and some studies have dealt with cylinders in forced transverse oscillation (e.g. [10]), but to the best knowledge of the authors heat transfer from an elastically supported cylinder has not yet been investigated.

In this study fluid flow around a circular cylinder in 1DoF free vibration is investigated using a numerical approach. Since, the currently applied in-house code has been newly extended to free oscillation cases; validation is required. The main objective of the current paper is to compare results obtained using the current code with those in the literature in order to validate the extended code. A second aim is to investigate the effect of reduced velocity on heat transfer and mechanical energy transfer between the cylinder and fluid.

COMPUTATIONAL METHOD

The non-dimensional governing equations for the two-dimensional, incompressible, constant property, Newtonian fluid flow around and heat transfer from a cylinder undergoing one-degree-of freedom (1DoF) free vibration are the two components of the Navier-Stokes equations – written in a non-inertial system fixed to the moving body, continuity equation, Poisson equation for pressure and energy equation. These are written in the following forms:

$$\frac{\partial u}{\partial t}+u\frac{\partial u}{\partial x}+v\frac{\partial u}{\partial y}=-\frac{\partial p}{\partial x}+\frac{1}{\mathrm{Re}}\left(\frac{\partial^2 u}{\partial x^2}+\frac{\partial^2 u}{\partial y^2}\right), \tag{1}$$

$$\frac{\partial v}{\partial t}+u\frac{\partial v}{\partial x}+v\frac{\partial v}{\partial y}=-\frac{\partial p}{\partial y}+\frac{1}{\mathrm{Re}}\left(\frac{\partial^2 v}{\partial x^2}+\frac{\partial^2 v}{\partial y^2}\right)-\frac{\mathrm{d}^2 y_0}{\mathrm{d}t^2}, \tag{2}$$

$$D=div\,\mathbf{v}=\frac{\partial u}{\partial x}+\frac{\partial v}{\partial y}=0, \tag{3}$$

$$\nabla^2 p=2\left(\frac{\partial u}{\partial x}\frac{\partial v}{\partial y}-\frac{\partial u}{\partial y}\frac{\partial v}{\partial x}\right)-\frac{\partial D}{\partial t}, \tag{4}$$

$$\frac{\partial \Theta}{\partial t}+u\frac{\partial \Theta}{\partial x}+v\frac{\partial \Theta}{\partial y}=\frac{1}{\mathrm{RePr}}\left(\frac{\partial^2 \Theta}{\partial x^2}+\frac{\partial^2 \Theta}{\partial y^2}\right). \tag{5}$$

The advantage of using a non-inertial system fixed to the moving body is that the grid has to be generated only once, not in every time step. In Eqs. (1)–(5) u, v are the non-dimensional velocity components, t is the non-dimensional time, p is the dimensionless pressure, $\mathrm{d}^2y_0/\mathrm{d}t^2$ is the non-dimensional acceleration of the cylinder in transverse direction, D is the dilation and $\Theta=(\tilde{\Theta}-\tilde{\Theta}_\infty)/(\tilde{\Theta}_w-\tilde{\Theta}_\infty)$ is the dimensionless temperature, where $\tilde{\Theta}_w$ and $\tilde{\Theta}_\infty$ are the temperature of the wall and of the fluid far from the cylinder, respectively. In these equations $\mathrm{Re}=U_\infty d/\nu$ is the Reynolds number; $\mathrm{Pr}=\rho\nu c_p/k$ is the Prandtl-number, where ρ is the fluid density; c_p

is the specific heat at constant pressure; and k is the thermal conductivity. The motion of the cylinder in the transverse direction is governed by the following non-dimensional equation [1]

$$\ddot{y}_0 + \frac{4\pi}{U^*}\zeta\dot{y}_0 + \left(\frac{2\pi}{U^*}\right)^2 y_0 = \frac{2C_L(t)}{\pi m^*}. \tag{6}$$

Here $m^*=4m/D^2\pi\rho$ is the mass ratio, where m is the mass of the cylinder; $U^*=U_\infty/f_nD$ is the reduced velocity, where f_n is the natural frequency of the system; ζ is the structural damping ratio; and C_L is the unsteady lift coefficient. In Eq. (6) y_0, $\dot{y}_0$, $\ddot{y}_0$ represent the dimensionless transverse displacement, velocity and acceleration of the cylinder.

The lift coefficient is defined as

$$C_L = \frac{2F_L}{\rho U_\infty^2 d}, \tag{7}$$

where F_L is the lift per unit length of the cylinder. The flow is strongly influenced by mechanical energy transfer E between the cylinder and the fluid. It is defined [11] as:

$$E = \int_0^T C_L\dot{y}\mathrm{d}t, \tag{8}$$

where T is the motion period. In this study heat transfer is also investigated. The local Nusselt number Nu – which is also a time dependent signal – can be obtained as

$$Nu = \frac{hd}{k} = -\left(\frac{\partial\Theta}{\partial R}\right)_w, \tag{9}$$

where h is the heat transfer coefficient and R is the dimensionless radius, and w refers to the cylinder wall.

In Fig. 1 the physical and computational domains are shown, where R_1 represents the cylinder radius and R_2 is the radius of the far field, where the flow is assumed to be undisturbed. For velocity and temperature Dirichlet-type and for pressure Neumann-type boundary conditions are applied on both R_1 and R_2.

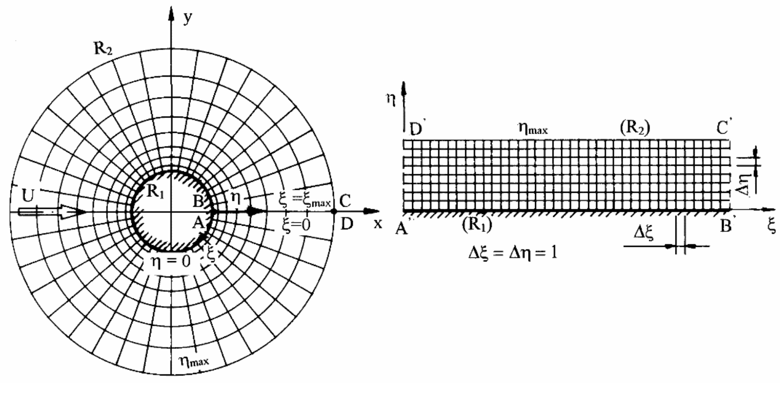

Figure 1
The physical and computational domains

In order to impose boundary conditions accurately, boundary-fitted coordinates are used. The physical domain is mapped into a rectangular computational domain applying mapping functions [11]. Due to the properties of the mapping functions, the grid on the physical plane is very fine in the vicinity of the cylinder surface and coarse in the far field, but the grid is equidistant throughout the computational domain. The transformed governing equations with the boundary and initial conditions are solved using finite difference method [11]. The space derivatives are discretized using fourth order schemes except for the convective terms which are approximated by a third order upwind difference scheme. Equations of motion (1) and (2), energy equation (5) and structural equation (6) are integrated explicitly, the Poisson equation (4) is solved using the successive over relaxation (SOR) method, and the continuity equation (3) is satisfied in every time step.

During the computations the radius ratio R_2/R_1=160 and the computational grid is characterized by grid points 360×292 (peripheral × radial) and the dimensionless time step Δt is 0.0005.

COMPUTATIONAL RESULTS

In this study flow around and heat transfer from an elastically supported cylinder is investigated using a newly extended computational code. In order to investigate its accuracy, a comparison of the results obtained from this code and the literature is carried out for 1DoF cylinder motion. Cylinder response, time-mean (TM), root-mean-square (rms) and peak values of lift and vorticity contours will be shown. Mechanical energy transfer and heat transfer results will also be presented.

The cylinder is restricted to oscillate only transverse to the main stream. Reynolds number, mass ratio, structural damping were chosen to be identical with the data in [6], i.e., Re=200, m^*=10 and ζ=0.01, respectively. The reduced velocity was varied between U^*=4–7. The maximum amplitude of the cylinder displacement y_{0max} and the peak value of the lift coefficient C_{Lmax} are shown in Fig. 2. As seen in the figure, very good agreement was found between the current results and those in [6].

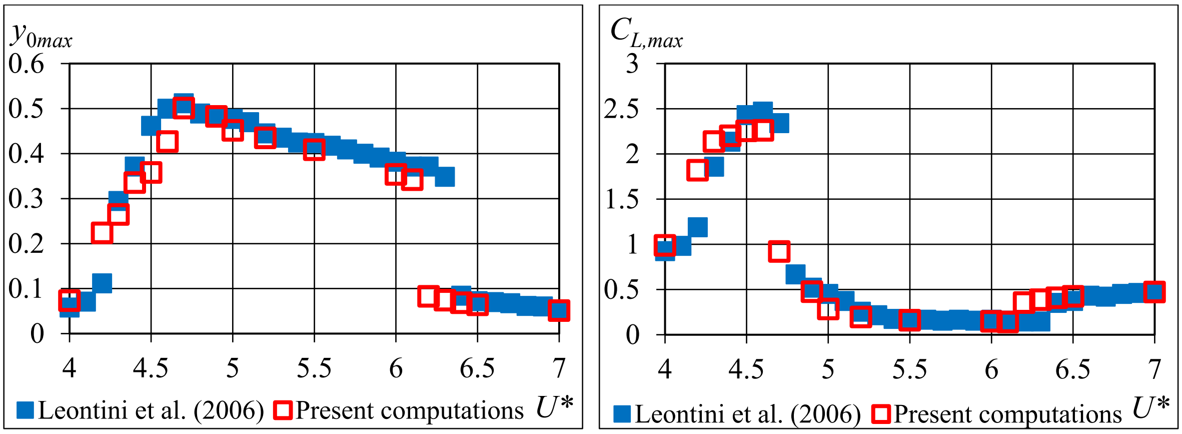

a) y_{0max} against U^* b) C_{Lmax} against U^*

Figure 2

Maximum oscillation amplitude (a) and peak value of lift coefficient (b) against reduced velocity at Re=200; m^*=10; ζ=0.01; comparison with Leontini et al. [6]

The investigated U^* range can be divided into four sub-regimes (1) $U^* < 4$: small-amplitude oscillation; (2) $4.3 < U^* < 4.7$: chaotic regime where the oscillation amplitude strongly varies; (3) $4.7 < U^* < 6.2$: slightly decreasing amplitudes; (4) $U^* > 6.2$: small-amplitude regime. These sub-regimes can also be observed in Fig. 2(b), where the peak values of C_L are presented.

The vortex shedding mode changes with reduced velocity, as seen in Fig. 3. Vortices at low U^* values – where the oscillation amplitude is small – are in single-row configuration (Fig. 3/a)). In the U^* domain of $4.7 < U^* < 5.9$ a double-row configuration can be observed. There is a phase shift between lift and transverse displacement which increases with U^* in the interval of $4.7 < U^* < 9.0$ ([6]). Due to this phase shift a shift can be observed in the vortex configurations shown in Figs. 3b) and 3c). With a further increase in U^* to $U^*=6.0$ the vortices are in a single row configuration again (Fig. 3/d)).

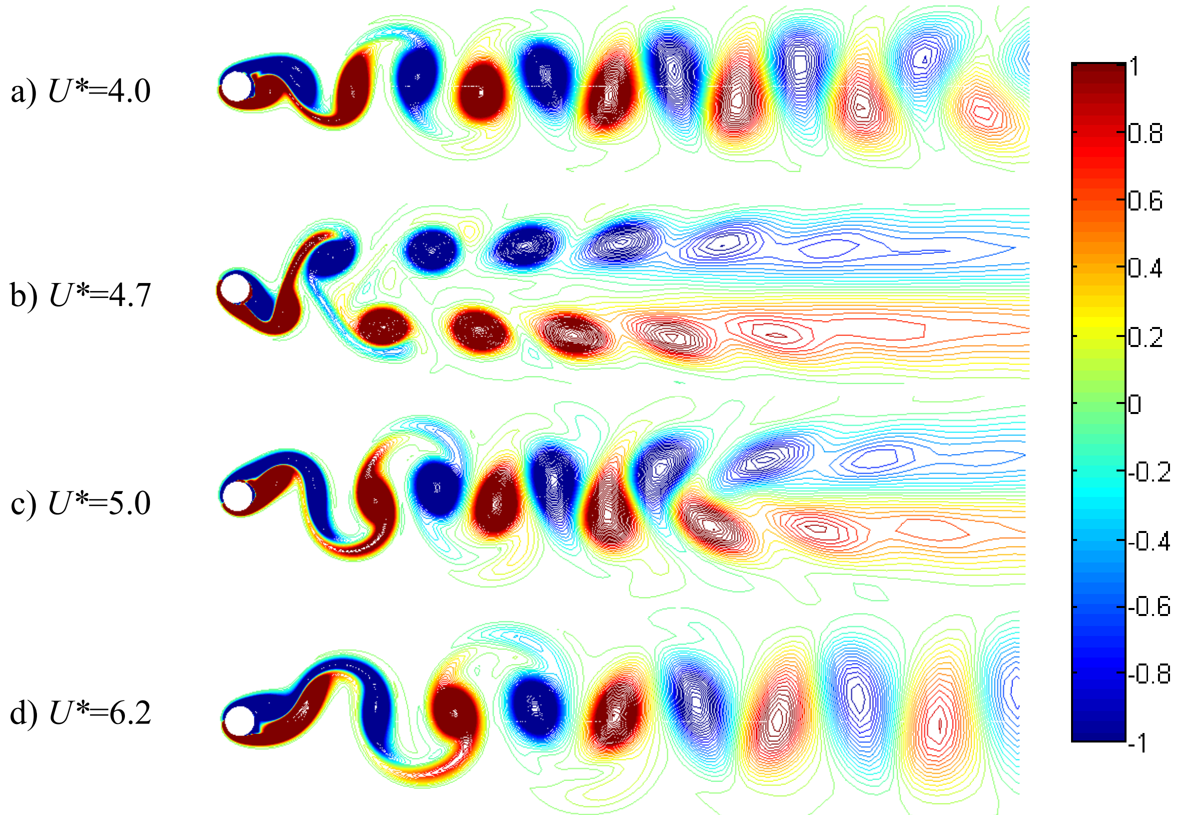

Figure 3
Vorticity contours for different reduced velocity values
at Re=200; $m^*=10$; $\zeta=0.01$ (at $t=800$)
a) single-row; b) double row; c) delayed double row; d) single-row

The mechanical energy transfer E between the oscillating body and the neighboring fluid is shown in Fig. 4. E is positive in the investigated U^* range, hence energy is transferred from the fluid to the cylinder. It can also be seen that the maximum value of E is at U^*~4.7 where the oscillation amplitude is the highest and that E is very small (near 0) when $U^* < 4$ or $U^* > 6.2$.

The mechanical energy transfer E (Fig. 4) and the time-averaged Nusselt number Nu against U^* (Fig. 5) display similar patterns. As expected, the maximum amount of heat is transferred from the fluid to the cylinder where the oscillation amplitude $y_{0\max}$ is at its peak (U^*~4.7). On the other hand, the TM value of averaged Nusselt number, defined as the average value of the local Nusselt number defined by Eq. (9) on the cylinder surface, drops about 7% compared to its peak value when U^* <4 or U^* > 6 (See Fig. 5a)). As seen in Fig. 5b), in these U^* domains the rms values of the averaged Nusselt number are very small.

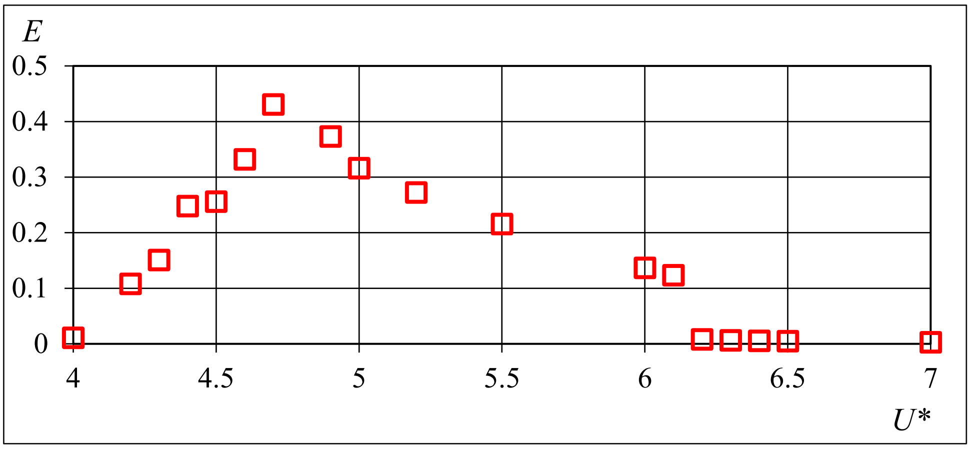

Figure 4
Mechanical energy transfer E vs. reduced velocity U^* at Re=200; m^*=10; ζ=0.01

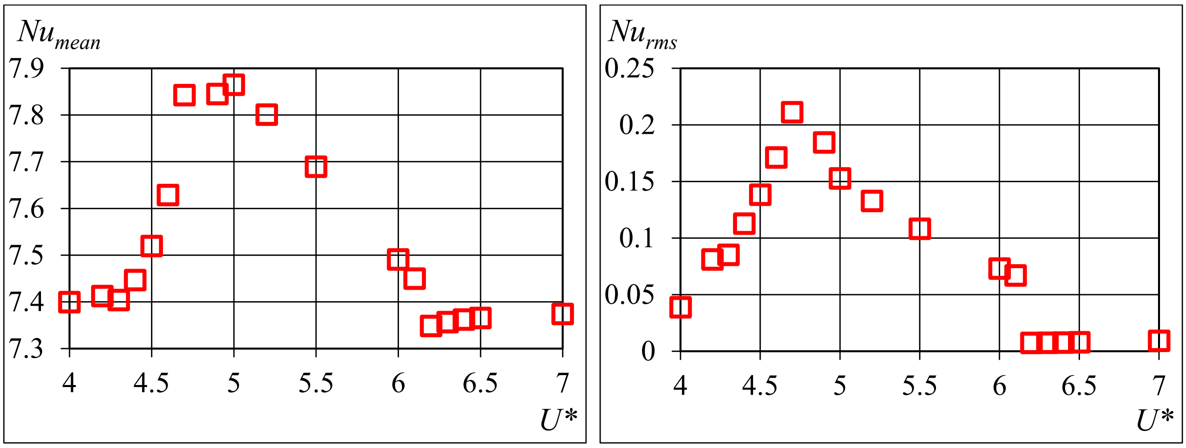

a) TM values of Nu b) rms values of Nu

Figure 5
TM and rms values of Nusselt number against reduced velocity at Re=200; m^*=10; ζ=0.01

CONCLUSIONS

This study deals with the numerical investigation of flow around and heat transfer from a cylinder undergoing one-degree-of freedom free vibration in transverse direction. Computations are carried out using a newly extended in-house code. For this reason the main objective of this study is to carry out a comparison between the results obtained from the current code and those in the literature. During the computations the mass ratio, structural damping and Reynolds number are kept at constant values of $m^*=10$, $\zeta=0.01$; Re=200 and the reduced velocity was varied between $U^*=4$ and 7. The maximum amplitude of cylinder oscillation $y_{0\max}$ and the peak value of lift coefficient C_{Lmax} are compared with those in the literature and very good agreement was observed. Vorticity contours are also shown for different reduced velocity values. Mechanical energy and heat transfer between the cylinder and the fluid were shown to increase with cylinder oscillation amplitude.

ACKNOWLEDGEMENT

This study was carried out as part of the EFOP-3.6.1-16-00011 "Younger and Renewing University – Innovative Knowledge City – institutional development of the University of Miskolc aiming at intelligent specialization" project implemented in the framework of the Széchenyi 2020 program. The realization of this project is supported by the European Union, co-financed by the European Social Fund.

REFERENCES

[1] KHALAK, A., WILLIAMSON, C.H.K.: **Motions, forces and mode transitions in vortex-induced vibrations at low mass-damping**. *Journal of Fluids and Structures* **13** (1999), 813–851.

[2] FENG, C.C.: **The measurement of vortex-induced effects in flow past stationary and oscillating circular and D-section cylinders**. Master thesis (1968), University of British Columbia, Vancouver, B.C., Canada

[3] BRIKA, D., LANEVILLE, A.: **Vortex-induced vibration of a long flexible circular cylinder**. *Journal of Fluid Mechanics* **250** (1993), 481–508.

[4] ANAGNOSTOPULOS, P., BEARMAN, P.: **Response characteristics of vortex-excited cylinder at low Reynolds numbers**. *Journal of Fluids and Structures* **6** (1992), 39–50.

[5] ANAGNOSTOPULOS, P.: **Numerical investigation of response and wake characteristics of a vortex excited cylinder in a uniform stream**. *Journal of Fluids and Structures* **8** (1994), 367–390.

[6] LEONTINI, J.S., THOMPSON, M.C., HOURIGAN, K.: **The beginning of branching behavior of vortex-induced vibration during two-dimensional flow**. *Journal of Fluids and Structures* **22** (2006), 857–864.

[7] BAHMANI, M.H., AKBARI, M.H.: **Effect of mass and damping ratios on VIV of a circular cylinder**. *Ocean Engineering* **37** (2010), 511–519.

[8] WANG, A.B., TRÁVNÍCEK, Z., CHIA, K.C.: **On the relationship of effective Reynolds number and Strouhal number for the laminar vortex shedding of a heated circular cylinder**. *Physics of Fluids* **12** (2000), 1401–1410.
[9] BARANYI, L.: **Computation of unsteady momentum and heat transfer from a fixed circular cylinder in laminar flow**. *Journal of Computational and Applied Mechanics* **4**(1) (2003), 13–25.
[10] CHENG, C-H, HONG, J-L.: **Numerical prediction of lock-on effect on convective heat transfer from a transversally oscillating cylinder**. *International Journal of Heat and Mass Transfer* **40** (1997), 1825–1834.
[11] BARANYI, L.: **Numerical simulation of flow around an orbiting cylinder at different ellipticity values**. *Journal of Fluids and Structures* **24** (2008), 883–906.